

# Importance of Interfacial Phenomena and Synergistic Effects in Lanthanide Cation Extraction by Dithiophosphinic Ligands: A Molecular Dynamics Study

Bernard Coupez, Christian Boehme, and Georges Wipff\*

Laboratoire MSM, Institut de Chimie, UMR CNRS 7551, Université Louis Pasteur, 4, rue B. Pascal, 67 000 Strasbourg, France

Received: March 24, 2003; In Final Form: June 12, 2003

According to molecular dynamics simulations, uncomplexed Cyanex-301-like ligands  $L^-$  and  $LH$  (derived from the dithiophosphinic acid  $R_2PS_2H$ ) and their  $EuL_3$  complexes are surface active. They adsorb at a water/oil interface, where “oil” is modeled by chloroform. It is shown that addition of neutral phosphoryl ligands such as TBP (tri-*n*-butyl phosphate) is necessary to promote the extraction of the complex, via two complementary mechanisms. First, gradual co-complexation of TBP, forming  $EuL_3(TBP)_n$  species, enhances the interfacial activity and the hydrophobicity of the lanthanide complex. Second, high concentrations of TBP are needed to saturate and modify the interface, leading to the migration of the  $EuL_3(TBP)_3$  complex to the oil phase. The effect of oil/water ratio is also investigated. At high ratio, one observes the formation of water-in-oil microdroplets onto which TBPs adsorb, while the complexes are fully extracted to the oil phase. These features make it possible to better understand synergistic and solvation effects in the assisted liquid–liquid extraction of lanthanide or actinide cations.

## Introduction

Phosphoryl-containing molecules represent an important class of ligands that are used to extract trivalent lanthanide and actinide cations from aqueous solutions to an organic (“oil”) phase.<sup>1–4</sup> The recently developed acidic sulfur derivatives of  $R_2PSSH$  type, like Cyanex-301 (Figure 1) and Modolo’s molecules ( $R$  = phenyl derivatives)<sup>5–7</sup> make it possible to separate Am/Eu from acidic solutions.<sup>8–11</sup> They can also extract toxic heavy cations or uranium to supercritical fluid phases that display marked analogies with classical organic liquids.<sup>12</sup> It is generally believed that sulfur ligands are softer bases than the oxygen analogues and interact somewhat better with actinides than with lanthanides, which are somewhat harder Lewis acids. Complexation of  $M^{3+}$  trivalent metals with the deprotonated  $R_2PS_2^-$  ligands yields  $M(R_2PS_2)_3$  complexes, which are neutral and can therefore be extracted without further charge compensation. According to XAFS studies, such complexes form in *n*-dodecane solution with trivalent ions such as  $Cm^{3+}$ ,  $Sm^{3+}$ , or  $Nd^{3+}$ .<sup>13</sup> It has been noticed, however, that the formation of the complex is not sufficient, and that extraction is promoted upon addition of other neutral oxygen-bearing co-extractants (e.g., alkyl phosphates, phosphine oxides, CMPO, or diamides) whose role is poorly understood.<sup>10, 11, 14, 15</sup>

In this context, we report molecular dynamics (MD) simulations on “Cyanex-301” complexes of a  $M^{3+}$  cation, and on the effect of solvent and/or additives on the hydrophobic/hydrophilic balance of the complex, with a particular focus on the water/oil interface, which is presumably the meeting region between the  $M^{3+}$  cations (initially in water) and the extractant molecules (initially in oil).<sup>16,17</sup> More specifically, we consider the (phenyl)<sub>2</sub>PS<sub>2</sub><sup>−</sup> ligand (hereafter noted  $L^-$ ; see Figure 1) in its uncomplexed  $L^-$  and  $LH$  forms, and its 1:3 neutral  $EuL_3$  complex with  $Eu^{3+}$ , an average-sized lanthanide cation, also similar in size to  $Am^{3+}$ . The effect of added phosphoryl-

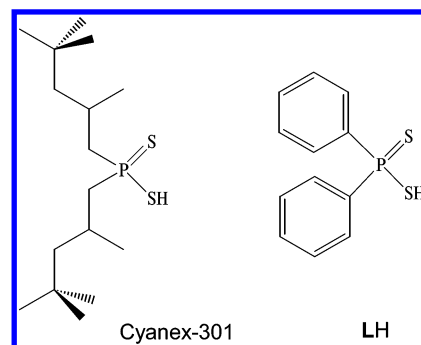


Figure 1. Dithiophosphinic extractants: Cyanex-301 and simulated ligand  $LH$ .

containing ligands is simulated by TBP (tri-*n*-butyl phosphate), forming  $EuL_3(TBP)_n$  complexes ( $n = 1–3$ ). The latter are considered without further additives, as well as in the presence of an excess of TBP, comparing two TBP concentrations (about 8 and 15% of the total volume). The characteristics of the simulated systems, noted **A** to **F**, are given in Table 1. The time evolution of  $L^-$ ,  $LH$ ,  $EuL_3$ , and  $EuL_3(TBP)_n$  systems is examined at a prebuilt water/oil interface, where “oil” is represented by chloroform. For the systems containing  $EuL_3(TBP)_3$  and an excess of TBP, we report mixing/demixing MD experiments, where “random” mixtures of water, oil, and the solute are first prepared, and their spontaneous evolution is then simulated at 300 K. Two important issues concern (i) the extent of water/oil separation and (ii) the behavior of the complexes and TBP molecules: Will they migrate to the organic phase where they are more soluble, or concentrate near the interface? What is the driving force for diffusing from the interface toward the oil phase? Another facet concerns the effect of relative water/oil ratio. Although the above systems will be simulated with similar volumes of both liquids, we decided to also model systems in which one liquid is in excess, to seek for possible

\* Corresponding author. E-mail: wipff@chimie.u-strasbg.fr.

TABLE 1: Characteristics of the Simulated Systems

	systems	$N_{\text{Chlor}} + N_{\text{WAT}}$	box ( $\text{\AA}^3$ )	time <sup>a</sup> (ns)
<b>A</b> <sub>0</sub>	9 LH	454 + 2050	40*40*(39+39)	0.5
<b>A</b> <sub>+-</sub>	9 L <sup>-</sup> H <sub>3</sub> O <sup>+</sup>	455 + 2051	40*40*(39+39)	0.5
<b>A</b> <sub>mix</sub>	5 L <sup>-</sup> H <sub>3</sub> O <sup>+</sup> , 4 LH	454 + 2050	40*40*(39+40)	0.5
<b>B</b>	ML <sub>3</sub> (M = La/Eu/ Yb)	307 + 1207	35*35*(30+35)	0.3
<b>C</b> <sub>1</sub>	EuL <sub>3</sub> (TBP) <sub>1</sub>	340 + 1449	37*35*(36+35)	1.0
<b>C</b> <sub>2</sub>	EuL <sub>3</sub> (TBP) <sub>2</sub>	333 + 1320	36*35*(37+33)	1.8
<b>C</b> <sub>3</sub>	EuL <sub>3</sub> (TBP) <sub>3</sub>	340 + 1143	37*36*(36+35)	0.8
<b>D</b>	9 EuL <sub>3</sub> (TBP) <sub>3</sub> + 30 TBP	606 + 2812	54*50*(39+38)	0.1/1.5/2.2
<b>E</b>	9 EuL <sub>3</sub> (TBP) <sub>3</sub> + 60 TBP	488 + 2319	51*46*(42+43)	0.1/1.0/4.5
<b>E</b> <sub>PME</sub>	9 EuL <sub>3</sub> (TBP) <sub>3</sub> + 60 TBP	488 + 2319	51*46*(42+43)	0.1/1.0/4.0
<b>E</b> <sub>cubic</sub>	9 EuL <sub>3</sub> (TBP) <sub>3</sub> + 60 TBP	488 + 2319	58*58*58	0.1/1.0/4.8
<b>F</b> <sub>1/1</sub>	9 EuL <sub>3</sub> (TBP) <sub>3</sub> + 60 TBP	488 + 2319	58*58*58	0.1/1.0/4.8
<b>F</b> <sub>1/2</sub>	9 EuL <sub>3</sub> (TBP) <sub>3</sub> + 60 TBP	854 + 727	58*58*58	0.1/0.9/1.6
<b>F</b> <sub>2/1</sub>	9 EuL <sub>3</sub> (TBP) <sub>3</sub> + 60 TBP	101 + 4454	58*58*58	0.1/1.1/1.5
<b>F</b> <sub>1/4</sub>	9 EuL <sub>3</sub> (TBP) <sub>3</sub> + 60 TBP	924 + 586	58*58*58	0.1/0.8/1.6

<sup>a</sup> The times are given for equilibration/mixing/demixing, respectively.

formation of water-in-oil or oil-in-water emulsions and gain insights into the distribution of the complexes.

## Methods

Classical molecular dynamics (MD) simulations have been performed in pure aqueous solution and at the water/"oil" interface using the modified AMBER5.1 software<sup>18</sup> with the following representation of the potential energy  $U$ :

$$U = \sum_{\text{bonds}} K_r(r - r_{\text{eq}})^2 + \sum_{\text{angles}} K_\theta(q - q_{\text{eq}})^2 + \sum_{\text{dihedrals}} \sum_n V_n(1 + \cos n\phi) + \sum_{i < j} \left( \frac{q_i q_j}{R_{ij}} - 2\epsilon_{ij} \left( \frac{R_{ij}^*}{R_{ij}} \right)^6 + \epsilon_{ij} \left( \frac{R_{ij}^*}{R_{ij}} \right)^{12} \right)$$

It is based on a fixed ball-and-stick representation of the system and accounts for the deformation of angles, bonds and dihedral angles, and for nonbonded interactions represented by 1-6-12 pairwise contributions. The water and chloroform solvents were represented explicitly at the molecular level with the TIP3P and OPLS models, respectively.<sup>19,20</sup> The La<sup>3+</sup>, Eu<sup>3+</sup>, and Yb<sup>3+</sup> cation parameters have been fitted from free energy hydration calculations<sup>21</sup> whereas the charges of the L<sup>-</sup> and LH forms of the ligand were derived from ESP ab initio HF calculations with the 6-31G\* basis set<sup>22</sup> and TBP charges were taken from ref 23. The other force field parameters for the solute were taken from the AMBER force field.<sup>24</sup> The nonbonded interactions were calculated with a residue based cutoff of 15 Å, considering each ligand as a single residue, and using a reaction field correction to the electrostatic interactions. We also performed tests with the particle mesh Ewald (PME) correction in three dimensions, which yield satisfactory results for systems of two-dimensional periodicity.<sup>25, 26</sup>

The interface was built as described in ref 27, starting with adjacent boxes of water and chloroform. The solutes were initially immersed at the interface, either as single complexes (systems **B** and **C**) or as a 3 × 3 grid of ligands (systems **A**<sub>0</sub>, **A**<sub>+-</sub>, and **A**<sub>mix</sub>) or of EuL<sub>3</sub>(TBP)<sub>3</sub> complexes (systems **D**–**F**). In systems **D** and **E**, the TBPs initially formed 2 and 4 parallel layers of 15 TBP each, respectively, parallel to the interface (Figure 2). The systems **F** contain the same solutes as **E**, but with different water/oil ratios. After 3000 steps of energy minimization and 50–200 ps of MD equilibration under a pressure of 1 atm, each MD was run at 300 K in the ( $N$ ,  $V$ ,  $T$ ) ensemble using 3D periodic boundary conditions. The trajectories were calculated with a time step of 2 fs in conjunction with SHAKE on the bonds of water and chloroform molecules and C–H

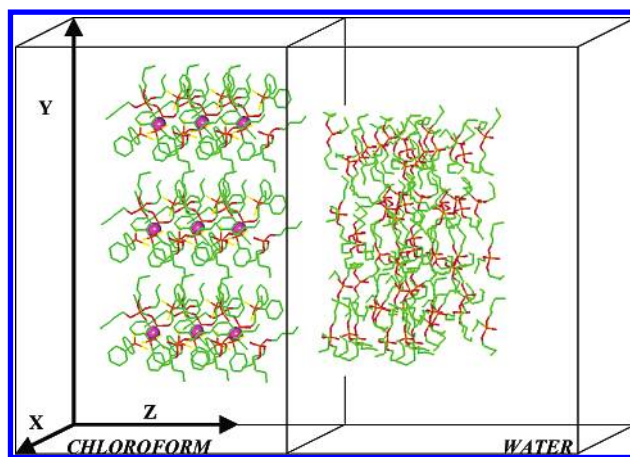


Figure 2. Schematic representation of the chloroform/water interface (solvent molecules not shown) with 60 TBPs and 9 EuL<sub>3</sub> complexes.

bonds of the solutes. The temperature was maintained constant by separately coupling the solvent and solute to thermal baths using the Berendsen algorithm<sup>28</sup> with a relation time of 0.2 ps.

The mixing/demixing experiments were performed on **D**–**F**, starting from equilibrated biphasic water/oil solutions. The mixing was achieved by increasing the temperature to 500 K and scaling down the electrostatic interactions by a factor of 100. Constraints of 10 kcal/mol were imposed on the molecular mechanics optimized Eu–S and Eu–O distances of the EuL<sub>3</sub> and EuL<sub>3</sub>(TBP)<sub>3</sub> complexes, to prevent their dissociation during the heating process and during the first 50 ps of the demixing process. The demixing step was initiated by resetting the temperature to 300 K and the dielectric constant to 1.0. The coordinates saved every 0.5 ps were carefully analyzed at the computer graphics system using our DRAW software, whereas more quantitative data (structural parameters, radial distribution functions, energy component analysis, density profiles) were obtained with the MDS software.<sup>29</sup> The position of the interface (when present) was dynamically defined as the intersection between the water and oil smoothed density curves, as in ref 30.

## Results

**1. Free Ligands and the EuL<sub>3</sub>(TBP)<sub>3</sub> Complexes Adsorb at the Water/"Oil" Interface.** The uncomplexed ligands are acidic and may exist in their neutral form LH, as well as in their deprotonated form L<sup>-</sup>, which are likely to dominate in the oil phase and aqueous phase, respectively. As the pK<sub>a</sub> of the acidic ligands at the interface is not known, we decided to consider three model systems of nine ligands at the interface,

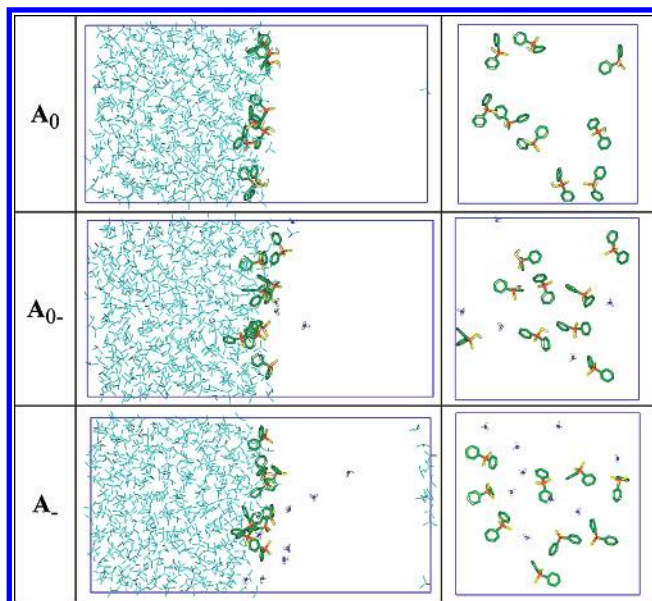


**Figure 3.** Free ligands at the interface: systems  $A_0$  (9 LH),  $A_{0-}$  (9  $L^-$ , 9  $H_3O^+$ ),  $A_{mix}$  (4 LH + 5  $L^-$ , 5  $H_3O^+$ ). Snapshots after 0.3 ns. The water molecules (right-hand side of the interface) are omitted for clarity. Right: slice 10 Å thick in the xy plane of the interface.

which are represented either (i) all in the LH form, (ii) all in the ionic  $L^- H_3O^+$  form, or (iii) as a mixture of 4 LH + 5  $L^- H_3O^+$  species. These systems are labeled  $A_0$ ,  $A_{0-}$ , and  $A_{mix}$ , respectively. According to our simulations, all ligands are surface-active (see Figure 3). The nine LH species remain adsorbed at the interface until the end of the dynamics, oscillating a few ångströms between the interface and chloroform. Some LH molecules have no contact with water and are completely surrounded by “oil”, whereas others are hydrogen bonded to  $H_2O$  molecules. As a result, the average interaction energies per LH molecule with water and chloroform are  $-25 \pm 2$  and  $-20 \pm 2$  kcal/mol, respectively, thus showing that these hydrophobic ligands, although more soluble in “oil” than in water, are attracted at the interface by specific interactions with water. The ionic  $L^-$  ligands are more hydrophilic than LH neutral but, after 0.5 ns of simulation, they also remain at the interface, albeit more on the water side. About half of the neutralizing  $H_3O^+$  cations diffused into the bulk water, whereas the other half remained at the interface, attracted by the negatively charged ligands, without forming hydrogen bonds with them. On the average, each  $L^-$  species interacts much more with water ( $-102 \pm 5$  kcal/mol) and somewhat less with chloroform (about  $-17 \pm 2$  kcal/mol) than does an LH molecule. Not surprisingly, in the  $A_{mix}$  system which combines the features of the  $A_0$  and  $A_{0-}$  ones, all ligands adsorb at the interface, but their concentration is too low to cover the interface (see Figure 3).

When the  $EuL_3$  complex was similarly simulated at the interface, it rapidly dissociated:  $Eu^{3+}$  moved to water, while the three  $L^-$  ligands remained at the interface. Dissociation resulted from the poor cation shielding by the ligands and from the resulting coordination of water molecules to  $Eu^{3+}$ . This is why in subsequent simulations on  $ML_3$  complexes (systems B) we decided to constrain the six M–S distances, to prevent dissociation and to investigate their interfacial behavior. After 0.3 ns of dynamics, the  $LaL_3$ ,  $EuL_3$ , and  $YbL_3$  complexes sit on the water side of the interface, retaining weak contacts with the organic phase via the phenyl rings of the ligands (Figure 4). As respectively three, three, and four  $H_2O$  molecules coordinate the metal in its first sphere, the complexes are much

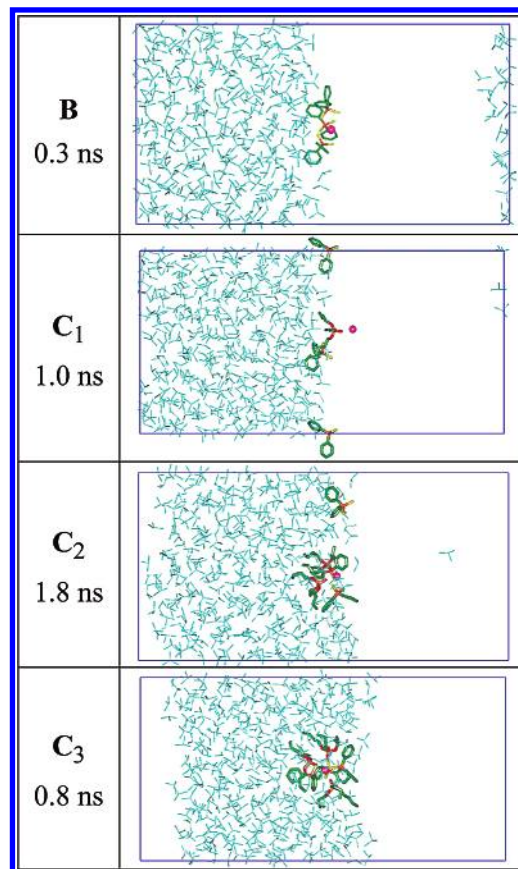


**Figure 4.** Systems B ( $EuL_3$  complex with six Eu–S constrained distances) and  $C_n$  ( $EuL_3(TBP)_n$  complexes free of constraints) at the interface. The water molecules (right-hand side) are omitted for clarity.

more attracted by water ( $-367 \pm 16$ ,  $-228 \pm 16$ , and  $-257 \pm 16$  kcal/mol, respectively, for  $M = La, Eu$ , and  $Yb$ ) than by chloroform ( $-32 \pm 10$ ,  $-54 \pm 10$ , and  $-47 \pm 10$  kcal/mol, respectively) and therefore cannot be extracted. The high affinity for water stems from a structural reorganization of the complexes at the interface, as compared to the gas phase: in the gas phase the three  $L^-$  ligands adopt a least repulsion “symmetrical” arrangement whereas, at the interface, they sit on the same side, pointing their aromatic groups to chloroform, thus forming a  $(L^-)_3Eu^{3+}$  dipole that is strongly attracted by the aqueous phase.

We next decided to test the effect of  $n$  additional TBP ligands on the stability of  $EuL_3$  at the interface (systems  $C_n$ ). The  $EuL_3(TBP)_1$  and  $EuL_3(TBP)_2$  complexes spontaneously dissociated, as europium was not shielded enough from water. The cation migrated to water, while all ligands adsorbed at the interface. This contrasts with the  $EuL_3(TBP)_3$  complex, which remained bound, sitting on the chloroform side of the interface (Figure 4). No water molecule coordinated to the cation and the average interaction energies of  $EuL_3(TBP)_3$  with water and chloroform were  $-60$  and  $-90$  kcal/mol, respectively. The attractions with water are reduced by  $\approx 170$  kcal/mol, compared to the  $EuL_3$  complex. They stem from the contributions of the three  $L^-$  and three TBP ligands ( $-100$  and  $-20$  kcal/mol, respectively), due to hydrogen-bonding interactions with the O(TBP) and S(L) atoms, whereas the  $Eu^{3+}$  contribution is clearly repulsive ( $+60$  kcal/mol), consistent with the efficient cation shielding. These simulations demonstrate the first important role of TBP-like ligands: they co-complex to the metal and, when the stoichiometry is appropriate, shield it enough from water-containing media to prevent its dissociation. It remains to be understood under which conditions the complex migrates from the interface to the oil phase. This is addressed in the next sections.



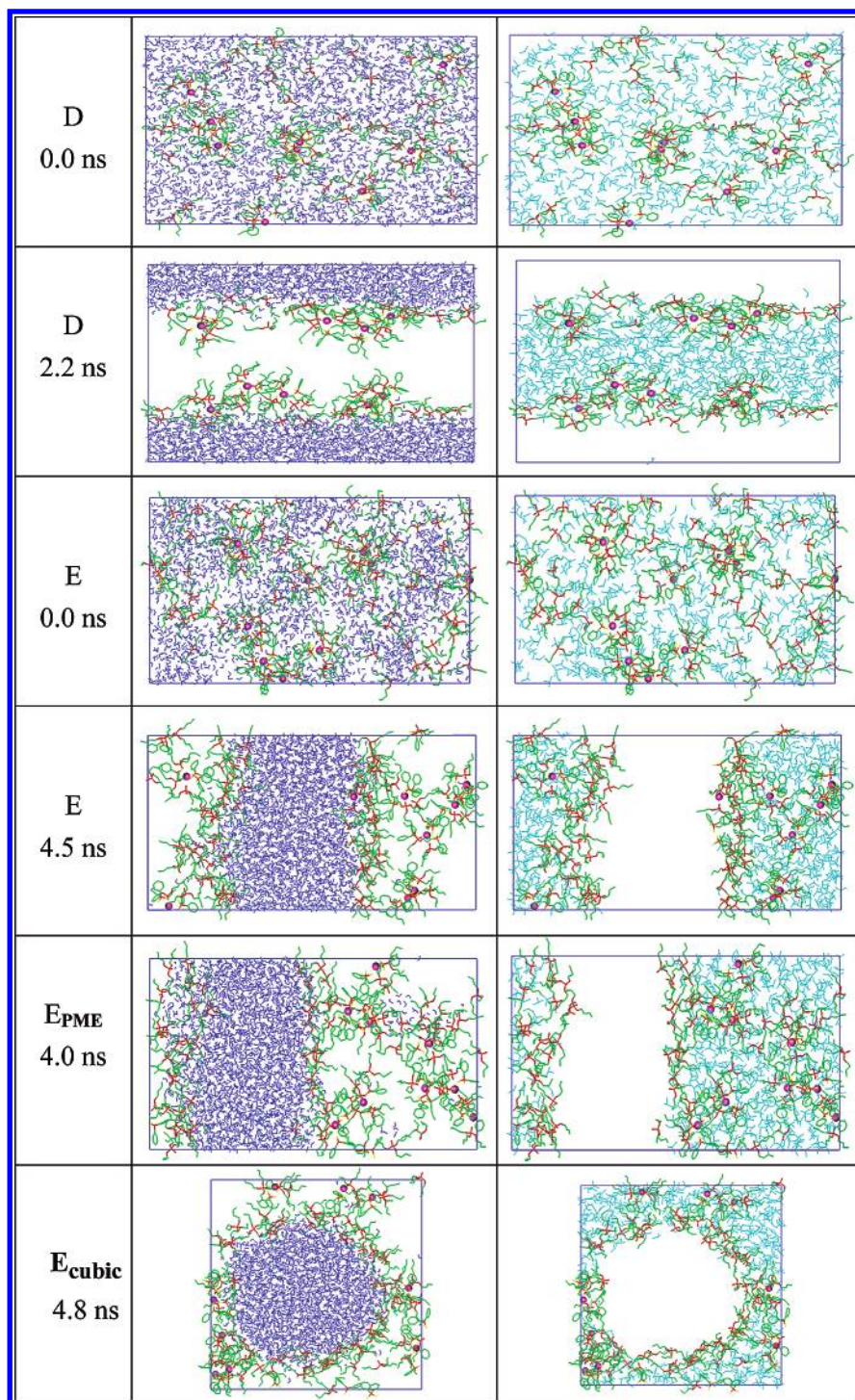


**Figure 5.** Demixing simulations of systems **D** (9  $\text{EuL}_3(\text{TBP})_3$  + 30 TBP) and **E** (9  $\text{EuL}_3(\text{TBP})_3$  + 60 TBP): with water and chloroform shown side by side, instead of superposed, for clarity.

**2. Demixing MD Experiments on the Water/“oil”/TBP/ $\text{EuL}_3(\text{TBP})_3$  Mixtures. Comparison of Two TBP Concentrations.** Experimentally, TBP or other oxygen-bearing synergistic molecules are added in large amounts, and a high concentration is a critical feature, as shown here, based on computer experiments.

We prepared mixed solutions containing 9  $\text{EuL}_3(\text{TBP})_3$  complexes, to which 30 TBP (system **D**), and 60 TBP molecules (**E**) were added. It can be seen in Figures 5 and S1 that at the end of the mixing stage (0 ns), the water, chloroform, and TBP molecules, and  $\text{EuL}_3(\text{TBP})_3$  complexes were “randomly” distributed in the simulation box. Although the constraints on the Eu–TBP and Eu–L distances were relieved after 50 ps, the

complexes remained bound during the whole demixing simulations. Shortly after the demixing was initiated, microaggregates of water formed and the complexes were sitting at the border between the two forming liquid phases. In less than one 1 ns, the water and chloroform phases were completely separated, and most of the solutes were sitting at the surface of water. The demixing was pursued up to 2.2 ns. There are interesting common features between the 30 and 60 TBP-containing systems. In both of them, the aqueous phase is neat, and does not contain TBP, chloroform, or  $\text{EuL}_3(\text{TBP})_3$  complexes, as expected from their hydrophobic character. Both demixed systems form two solvent slabs separated by water/“oil” interfaces.



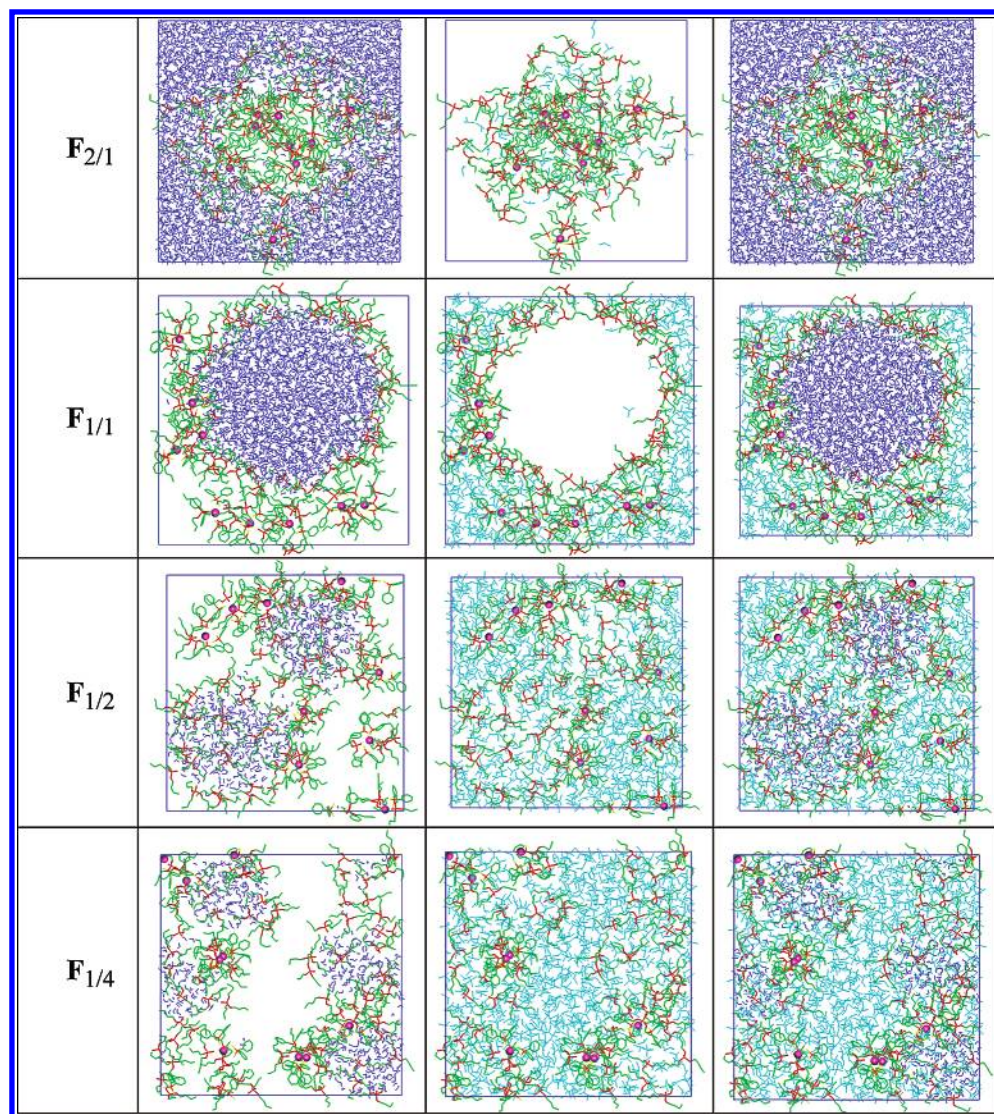


**Figure 6.** Demixing simulations of systems **F**, containing 9  $\text{EuL}_3(\text{TBP})_3$  + 60 TBP molecules in a “cubic box” at different water/oil ratios (1/1, 2/1, 1/2, and 1/4). Snapshots at 1.5 ns. See comments in Figure 4.

In system **D**, the interfaces are nearly planar on the average. TBP molecules and  $\text{EuL}_3(\text{TBP})_3$  complexes sit on the chloroform side of the interfaces, forming concentrated disordered arrangements. This is consistent with the surface activity of TBP itself<sup>23,31</sup> and of the  $\text{EuL}_3(\text{TBP})_3$  complexes observed above. The hydrophobic character of the complexes can be seen from the fact that two of them have no direct contact with the interface and can therefore be considered as “extracted”, whereas the seven other ones adsorb at the interface.

When the TBP concentration is doubled (system **E** with 60 TBPs), demixing is much slower and, after 2 ns, still not completed (Figures 5 and S2). There are no solutes in the aqueous phase, whereas the “oil” phase now contains a humid mixture of TBPs and about half of the complexes. The other half of the complexes sit on the oil side of the interface. Extraction is thus enhanced, compared to the **D** system. Note that the interface is very rough and irregular, which contrasts with its more planar appearance at lower TBP concentrations.<sup>23,32</sup> After 2 ns, the interface is “horizontal”, i.e., has a larger surface, and is a priori less stable than a smaller “vertical interface”. Indeed, pursuing the dynamics for another 2.5 ns leads to complete phase separation and formation of two “vertical” interfaces covered by TBP molecules and only one  $\text{Eu}(\text{TBP})_3$  complex (Figure 5). We notice that the latter lost its

$\text{L}^-$  ligands during the dynamics and thus became less hydrophobic than the saturated ones. All other complexes are extracted to the oil phase without any contact with water.

On the methodological side, we decided to investigate the effect of long-range forces and simulated the demixing of the **E** system using the Ewald summation method. The  $\text{E}_{\text{PME}}$  results (Figures 5 and S3) show that, after 4 ns, the two phases are separated and form two “flat” interfaces. They are quite irregular, and again partly covered by TBPs, which adopt more “random” orientations than in diluted conditions.<sup>23,32</sup> The aqueous phase is neat and the most interesting result, in the context of assisted ion extraction, is that all complexes are extracted to a “humid” organic phase that contains about 50 water molecules.

We also decided to investigate the role of the solvent box shape and forced the final **E** simulation box to become cubic, by stepwise changing its dimensions along a MD simulation at constant volume (system  $\text{E}_{\text{cubic}}$ ). This led to a spectacular reorganization and self-aggregation of water, which formed a cylindrical phase at the center of the cube (Figure 5). The aqueous phase remained “neat” and most TBPs adsorbed at the cylindrical interface. The most important result was again the extraction of most of the complexes into the oil phase, while the others retained loose contacts with the interface. When

compared to the **C**<sub>3</sub> and **D** simulations, the **E** and **E**<sub>cubic</sub> simulations thus show that, when the TBP concentration is high enough, the complexes are expelled from the interface to the oil phase.

**3. Demixing Experiments on the Water/“oil”/TBP/EuL<sub>3</sub>-(TBP)<sub>3</sub> Mixtures: Comparison of Different Water/“Oil” Ratios.** In this section, we compare the phase separation of several solutions **F** (characterized in Table 1 and shown in Figure 6), all containing 60 TBP and 9 EuL<sub>3</sub>(TBP)<sub>3</sub> neutral solutes, but at different water/oil (“w/o”) volume ratios. They are noted **F**<sub>w/o</sub>, where w/o are approximate integer numbers for simplicity. Thus, **F**<sub>1/1</sub> has in fact the same content as **E** (about 50% of each liquid), whereas **F**<sub>2/1</sub> contains an excess of water and **F**<sub>1/2</sub> and **F**<sub>1/4</sub> contain an excess of oil. Note that the shape of the simulation box is now cubic, to avoid the possible formation of two interfaces. In all cases, the starting systems were completely mixed with the solutes randomly dispersed in the solution. Upon demixing, the **F**<sub>1/1</sub> system led to a cylindrical phase as in the **E**<sub>cubic</sub> simulation, showing that the sampling is sufficient. When water is in excess (**F**<sub>2/1</sub>), all chloroform and TBP molecules rapidly condensed in a single irregular oil-in-water “droplet”. There is significant solvent mixing at the boundaries where one finds most of the complexes and some disordered TBP molecules. This contrasts with the **F**<sub>1/2</sub> and **F**<sub>1/4</sub> systems which formed water-in-oil microdroplets, however without condensing to a single water phase after 1.5 ns of MD demixing simulation. The complete phase separation of a diluted system with a w/o ratio near unity generally proceeds faster (<0.5 ns).<sup>27,32</sup> In **F**<sub>1/2</sub> and **F**<sub>1/4</sub> systems, there is no strong driving force for further water condensation, as the water droplets are covered by TBP molecules, and condensation would release these TBPs to the oil phase, therefore resulting in a loss of hydrogen-bonding interactions with water. The number and size of droplets depend on the w/o ratio, though. In the **F**<sub>1/2</sub> system, two water droplets of about 15 Å diameter formed, whereas in the **F**<sub>1/4</sub> system, water formed four “spherical” droplets of ≈10 Å diameter after 2.7 ns, surrounded by TBP molecules. Most of the other TBPs solubilized in the oil phase, sometimes linked by dynamically exchanged water. Concerning the EuL<sub>3</sub>(TBP)<sub>3</sub> complexes, they are *all* immersed in the oil phase, and can thus be considered as extracted from the aqueous medium. Thus, comparison of the **F**<sub>1/1</sub> to the **F**<sub>1/2</sub> and **F**<sub>1/4</sub> systems somewhat reflects expected trends in a liquid–liquid extraction experiment and clearly depicts the evolution from a well-defined interface between the two phases, to water-in-oil microemulsions and to humid oil, leading to the extraction of the complexed cation.

## Discussion and Conclusion

We report a series of molecular dynamics experiments on model systems to understand under which circumstances highly hydrophilic trivalent cations can be extracted from water to an oil phase by dithiophosphinic ligands. The oil phase was modeled by chloroform for convenience, due to its shorter relaxation time, compared to long chain linear alkanes. Chloroform is classically used for solvent extraction purposes,<sup>33</sup> and its choice is further validated by the fact that extraction experimentally proceeds to aromatic solvents (toluene, kerosene),<sup>5,8,14,34</sup> as well as to aliphatic ones (like TPH, which is a mixture of hydrocarbons, or dodecane),<sup>11,35</sup> indicating that the precise nature of the oil phase is not crucial. In our study, the synergistic agent (co-extractant) is modeled by TBP, which is used experimentally and well-documented in terms of computations at interfaces.<sup>32,36</sup> However, a large number of oxygen-bearing ligands (e.g., phosphoryl derivatives, monoamides,

diamides)<sup>10,11</sup> can be used as well, modulating the extraction efficiency and the lanthanide vs actinide extraction selectivity. The cation is modeled by trivalent europium, whose size is intermediate between La<sup>3+</sup> and Yb<sup>3+</sup>, and similar to Am<sup>3+</sup>. An important facet, not addressed in this paper, concerns the nature and structure of its first coordination shell, and theoretical approaches addressing this issue have to properly describe the nature of metal–ligand bonds, and to take into account the electron reorganization (polarization, charge transfer) as a function of the cation, the ligand(s), medium, and dynamics. See for instance the quantum mechanical study of ref 37. Our main focus is on solvent and synergistic effects on the assisted ion extraction process, using an explicit representation of the key partners involved in the process: the complexes, additional ligands or co-complexants, and the water and oil solvents.

For this purpose, we use a force field approach, with a 1-6-12 pairwise additive representation of nonbonded interactions, as in other simulations at interfaces (see e.g., refs 38–42). It does not mean that electronic reorganization effects are negligible. The most important ones concern the EuL<sub>3</sub>(TBP)<sub>n</sub> complex itself, due to the high charge of the metal and the charge and polarizability of the ligands. We note, however, that with our simple force field, the extracted complex has the common coordination numbers of nine for europium, with a 1:3 metal:ligand ratio observed experimentally, which is satisfactory. As concerns the solvents, the 1-6-12 potentials fitted on bulk water properties tend to overestimate the polarity of water at the interface<sup>43,44</sup> and also underestimate, e.g., the surface activity of soft ions.<sup>45,46</sup> The problem studied here mostly involves neutral solutes (TBP, the EuL<sub>3</sub> complex, and its TBP adducts) at the interface, for which solvent polarization effects should be less important than for “naked” ions. Accounting of electronic reorganization effects is certainly desirable but requires quantum mechanical methods, and the size and time scales involved in the studied systems presently prevent using CP-MD methods. As an alternative, one could use classical MD simulations with explicit atomic polarization, based on consistent calibration of atomic charges and polarizabilities. This is beyond the scope of our study, which is more qualitative and does not purport to quantitatively reproduce, e.g., thermodynamic properties, such as the partition coefficient of all partners, and surface tensions. The positive side of the force field model used is that it probably overestimates the hydrophilicity of the complex near the interface, in relation with the somewhat exaggerated dipole moment of water. Thus, the conclusion according to which, at sufficient TBP concentrations, the complex is extracted to oil, should be strengthened further by using polarizable solvent models with which water near the interface is less polar.

Other computational issues concern the choice of (*N*, *V*, *T*) thermodynamic ensemble for these computer experiments.<sup>47–50</sup> Alternatives, like (*N*, *P*, *T*) or (*N*, *γ*, *T*) ensembles, might be considered as well, possibly modifying the interfacial pressure and detailed distribution of the adsorbed species. We note that the mixing–demixing simulations correspond to systems out of equilibrium, for which control and interpretation of thermodynamic quantities is questionable. For related interfacial systems,<sup>51</sup> we also tested the effect of volume reduction and found no marked changes, as far as the interfacial distribution of extractant molecules is concerned. We decided however, to simulate two important systems, **E** and **E**<sub>cubic</sub> for 1 ns in the (*N*, *P*, *T*) conditions, starting at the end of the (*N*, *V*, *T*) simulations. The final results show minor volume variations (–3% and –2%, respectively) and very similar distributions of the solvents and the solutes (see Figure S4), indicating that our results do not



critically depend on the choice of thermodynamic ensemble. Other simulation issues, like the use of 3D periodicity and the treatment of long-range forces,<sup>25,52</sup> may also quantitatively affect the results, but we believe that overall structural features and their evolution from one system to the other is meaningful, as supported by our comparison of reaction field vs Ewald results.

Our approach is to consistently simulate systems of increasing complexity and concentration of synergistic ligands, with the aim to obtain microscopic views of the solutes in water–oil mixtures. Stepwise increase of TBP concentration reveals several important facets of synergism by oxygen-bearing ligands: (i) They co-complex the metal, therefore preventing additional water coordination to the complex, which becomes hydrophobic. (ii) As surface active molecules, they adsorb at the water–oil interface, the surface tension of which is decreased, therefore facilitating the interface crossing. Large amounts of synergistic ligands are necessary for promoting the migration of the complexes from the interface to the “oil” phase. In principle, the same effects could be achieved by an excess of uncomplexed Cyanex ligands as well, but the latter should be less efficient than oxygenated ligands for two reasons: (i) Their sulfur atoms may be too bulky to coordinate the ML<sub>3</sub> moiety and (ii) they are likely to be less surface-active than oxygen-bearing extractants, in agreement with the lower dipole moment and hydrogen-bonding capabilities. Another important related feature, not addressed in this study, concerns the ion-binding selectivity. It is indeed generally believed that the sulfur atoms favor actinide(III) over lanthanide(III) complexation. Co-complexation of synergistic harder ligands may be an additional source of selectivity, via their basicity and, most importantly, changes in steric effects in the first coordination shell of the metal.<sup>37</sup> Beyond the studied lanthanide ion extraction by dithiophosphinic ligands, our results more generally show the importance of collective “supramolecular” organization in water/oil mixtures, interfaces, and heterogeneous solutions.<sup>53–55</sup>

**Acknowledgment.** We are grateful to EEC and PRACTIS for support, and to IDRIS, CINES, and Université Louis Pasteur for allocation of computer resources and EEC (Contract F1KW-CT-2000-0088) for support. G.W. thanks G. Modolo and A. Geist for stimulating discussions.

**Supporting Information Available:** Figures S1–S4 of demixing simulation snapshots. This material is available free of charge via the Internet at <http://pubs.acs.org>.

## References and Notes

- Nash, K. L. *Solv. Extract. Ion Exch.* **1993**, *11*, 729–768.
- Nash, K. L.; Barrans, R. E.; Chiarizia, R.; Dietz, M. L.; Jensen, M. P.; Rickert, P. G. *Solv. Extract. Ion Exch.* **2000**, *18*, 605–631.
- Choppin, G. R.; Nash, K. L. *Radiochim. Acta* **1995**, *70/71*, 225–236.
- Rozen, A. M. *J. Radioanal. Nucl. Chem., Articles* **1990**, *143*, 337–355.
- Modolo, G.; Odoj, R. *Solv. Extract. Ion Exch.* **1999**, *17*, 33–53.
- Modolo, G.; Odoj, R. *Proceedings of the International Information Exchange Meeting on Actinide and Fission Product Partitioning and Transmutation, 5th* **1998**, 141–151.
- Modolo, G.; Odoj, R. *J. Alloys Compd.* **1998**, *271–273*, 248–251.
- Jarvinen, G.; Barrans, R.; Schroeder, N. C.; Wade, K.; Jones, M.; Smith, B.; Mills, J.; Howard, G.; Freiser, H.; Muralidharan, S. In *Separations of Elements*; Nash, K. L., Choppin, G. R., Eds.; Plenum Press: New York, 1995; pp 43–62.
- Hill, C.; Madic, C.; Baron, P.; Ozawa, M.; Tanaka, Y. *J. Alloys Compd.* **1998**, *271–273*, 159–162.
- Ionova, G.; Ionov, S.; Rabbe, C.; Hill, C.; Madic, C.; Guillaumont, R.; Modolo, G.; Krupa, J.-C. *New J. Chem.* **2001**, *25*, 491–501.
- Ionova, G.; Ionov, S.; Rabbe, C.; Hill, C.; Madic, C.; Guillaumont, R.; Krupa, J. C. *Solv. Extract. Ion Exch.* **2001**, *19*, 391–414.
- Lin, Y.; Liu, C.; Wu, H.; Yak, H. K.; Wai, C. M. *Ind. Eng. Chem. Res.* **2003**, *42*, 1400–1405.
- Jensen, M. P.; Bond, A. H. *J. Am. Chem. Soc.* **2002**, *124*, 9870–9877.
- Wang, X.; Zhu, Y.; Jiao, R. *J. Radioanal. Nucl. Chem.* **2002**, *251*, 487–492.
- Geist, A.; Weigl, M.; Gompfer, K. *Sep. Sci. Technol.* **2002**, *15*, 3369–3390.
- Watarai, H. *Trends Anal. Chem.* **1993**, *12*, 313–318.
- Prochaska, K. *Adv. Colloid Interface Sci.* **2002**, *95*, 51–72.
- Case, D. A.; Pearlman, D. A.; Caldwell, J. C.; Cheatham, T. E., III; Ross, W. S.; Simmerling, C. L.; Darden, T. A.; Merz, K. M.; Stanton, R. V.; Cheng, A. L.; Vincent, J. J.; Crowley, M.; Ferguson, D. M.; Radmer, R. J.; Seibel, G. L.; Singh, U. C.; Weiner, P. K.; Kollman, P. A. *AMBER5, University of California, San Francisco* **1997**.
- Jorgensen, W. L.; Chandrasekhar, J.; Madura, J. D.; Impey, R. W.; Klein, M. L. *J. Chem. Phys.* **1983**, *79*, 926–936.
- Jorgensen, W. L.; Briggs, J. M.; Contreras, M. L. *J. Phys. Chem.* **1990**, *94*, 1683–1686.
- van Veggel, F. C. J. M.; Reinhoudt, D. *Chem. Eur. J.* **1999**, *5*, 90–95.
- Boehme, C.; Wipff, G. *Chem. Eur. J.* **2001**, *7*, 1398–1407.
- Beudaert, P.; Lamare, V.; Dozol, J.-F.; Troxler, L.; Wipff, G. *Solv. Extract. Ion Exch.* **1998**, *16*, 597–618.
- Cornell, W. D.; Cieplak, P.; Bayly, C. I.; Gould, I. R.; Merz, K. M.; Ferguson, D. M.; Spellmeyer, D. C.; Fox, T.; Caldwell, J. W.; Kollman, P. A. *J. Am. Chem. Soc.* **1995**, *117*, 5179–5197.
- Spohr, E. *J. Chem. Phys.* **1997**, *107*, 6342–6348.
- Crozier, P. S.; Rowley, R. L.; Spohr, E.; Henderson, D. *J. Chem. Phys.* **2000**, *112*, 9253–9257.
- Muzet, N.; Engler, E.; Wipff, G. *J. Phys. Chem. B* **1998**, *102*, 10772–10788.
- Berendsen, H. J. C.; Postma, J. P. M.; van Gunsteren, W. F.; DiNola, A. *J. Chem. Phys.* **1984**, *81*, 3684–3690.
- Engler, E.; Wipff, G. In *Crystallography of Supramolecular Compounds*; Tsoucaris, G., Ed.; Kluwer: Dordrecht, The Netherlands, 1996; pp 471–476.
- Lauterbach, M.; Engler, E.; Muzet, N.; Troxler, L.; Wipff, G. *J. Phys. Chem. B* **1998**, *102*, 225–256.
- Sagert, N. H.; Lee, W.; Quinn, M. J. *Can. J. Chem.* **1979**, *57*, 1218.
- Baaden, M.; Berny, F.; Muzet, N.; Troxler, L.; Wipff, G. in *Calixarenes for Separation*; Lumetta, G., Rogers, R., Gopalan, A., Eds.; ACS Symposium Series 757; American Chemical Society: Washington, DC, 2000; pp 71–85.
- Izatt, R. M.; Clark, G. A.; Bradshaw, J. S.; Lamb, J. D.; Christensen, J. J. *Sep. Purif. Methods* **1986**, *15*, 21–72.
- Zhu, Y. *Radiochim. Acta* **1995**, *68*, 95–98.
- Jensen, M. P.; Bond, A. H. *Radiochim. Acta* **2002**, *90*, 205–209.
- Baaden, M.; Schurhammer, R.; Wipff, G. *J. Phys. Chem. B* **2002**, *106*, 434–441.
- Boehme, C.; Wipff, G. *Inorg. Chem.* **1999**, *38*, 5734–5741.
- Benjamin, I. *Chem. Rev.* **1996**, *96*, 1449–1475.
- Spohr, E.; Heinzinger, K. *Electrochim. Acta* **1988**, *33*, 1211–1222.
- Fernandes, P. A.; Cordeiro, M. N. D. S.; Gomes, J. A. N. F. *J. Phys. Chem. B* **1999**, *103*, 8930–8939.
- Wilson, M. A.; Pohorille, A. *J. Am. Chem. Soc.* **1996**, *118*, 6580–6587.
- Schweighofer, K. J.; Essmann, U.; Berkowitz, M. *J. Phys. Chem. B* **1997**, *101*, 10775–10780.
- Chang, T. M.; Dang, L. X. *J. Chem. Phys.* **1995**, *104*, 6772–.
- Dang, L. X.; Chang, T. *J. Chem. Phys.* **1997**, *106*, 8149–8159.
- Dang, L. X.; Chang, T.-M. *J. Phys. Chem. B* **2002**, *106*, 235–238.
- Jungwirth, P.; Tobias, D. J. *J. Phys. Chem. B* **2002**, *106*, 6361–6373.
- Zhang, Y.; Feller, S. E.; Brooks, B. R.; Pastor, R. W. *J. Chem. Phys.* **1995**, *103*, 10252.
- Feller, S. E.; Zhang, Y.; Pastor, R. W. *J. Chem. Phys.* **1995**, *105*, 4871.
- Tieleman, D. P.; Berendsen, H. J. C. *J. Chem. Phys.* **1996**, *105*, 4871–4880.
- Alejandre, J.; Tildesley, D. J.; Chapela, G. A. *J. Chem. Phys.* **1995**, *102*, 4574–4583.
- Vayssière, P.; Wipff, G. *Phys. Chem. Chem. Phys.* **2003**, *5*, 127–135.
- Dominguez, H.; Smodyrev, A. M.; Berkowitz, M. L. *J. Phys. Chem. B* **1999**, *103*, 9582–9588.
- Osseo-Asare, K. *Adv. Colloid Interface Sci.* **1991**, *37*, 123–173.
- Smit, B.; Hilbers, P. A. J.; Esselink, K.; Rupert, L. A. M.; van Os, N. M.; Schlijper, A. G. *J. Phys. Chem.* **1991**, *95*, 6361–6368.
- Erlinger, C.; Belloni, L.; Zemb, T.; Madic, C. *Langmuir* **1999**, *15*, 2290–2300.